Introduction to Proton Detection in Biological Samples under Ultra-Fast Magic Angle Spinning

Venita Daebel

Bruker BioSpin GmbH, Rheinstetten, Germany

Protons are characterized by having a natural abundance of more than 99.9 %, as well as a high gyromagnetic ratio. These attributes provide much greater detection sensitivity than those of ^{13}C or ^{15}N, making ^{1}H-detected NMR spectroscopy very attractive, not just for solution NMR.[1-6]

Soluble samples benefit from the fact that unwanted dipolar couplings are cancelled out by molecular tumbling, a feature that insoluble molecules lack. As a result, a strong network of homonuclear proton dipolar couplings dramatically broadens the linewidth of any ^{1}H signal in solid-state NMR.

Two approaches especially have been shown to overcome this obstacle; sample preparation using perdeuteration-reprotonation to dilute the dense proton network[1-3], and the use of increased magic angle spinning (MAS) speeds in the order of 60 to 111 kHz (Figure 1).[3,5]

In collaboration with Guido Pintacuda and co-workers, Bruker BioSpin presents three basic ^{1}H-detected pulse programs ('pulprog') that allow initial protein backbone assignment under fast MAS[3] :

Figure 1

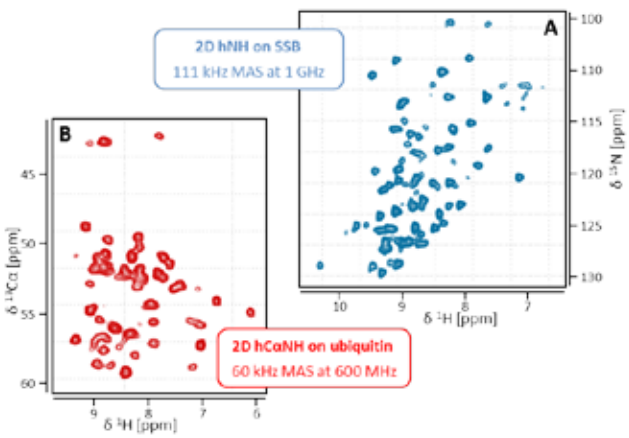

Figure 1: (A) 2D ^{1}H-detected hNH spectrum (blue) of a u-[^{13}C,^{15}N]-labeled and 100% ^{1}H-back-exchanged SSB sample recorded within 30 min on a Bruker 1GHz spectrometer at 111 kHz MAS (Bruker 0.7 mm probe). (B) 2D ^{1}H-detected hCαNH spectrum (red) of ubiquitin (same labeling scheme) recorded within 65 min on a Bruker 600 MHz spectrometer at 60 kHz MAS.

1. hNH: 1D and 2D, Figures 1A and 3, pulprog: hNH2D.dcp
2. hCαNH: 1D-3D , Figures 1B and 4, pulprog: hCaNH3D.tcp
3. hCONH: 1D-3D , Figures 4 and 6B, pulprog: hCONH3D.tcp

Introduction

Depending on the sample properties, ^{1}H dipolar couplings can be in the order of several tens of kHz. The higher the MAS rate, the more attenuated the unwanted ^{1}H dipolar couplings will be (Figure 2, black), resulting in better resolved ^{1}H signals and allowing for the use of polarization transfer using scalar couplings[7] (Figure 2, orange).

In the past, solid-state NMR was limited to moderate MAS rates (≤25 kHz) by probe designs. Fortunately, recent developments have seen a move towards small rotor sizes – for example Bruker 1.9, 1.3 and 0.7 mm H/C/N probes – allowing the use of fast (40 to 60 kHz) or even ultra-fast (60 to 111 kHz) MAS.[3,5]

Under these conditions, low power irradiation for heteronuclear decoupling and selective heteronuclear cross polarization (CP)[8] is efficient, minimizing RF irradiation-induced sample heating.

Another approach to reducing ^{1}H dipolar couplings targets the dilution of the dense ^{1}H network.[1] During sample preparation, the protein of interest is expressed in a perdeuterated growth medium. When the sample is subsequently incubated with a defined $^{2}H_2O$:$^{1}H_2O$ buffer, exchangeable sites such as amide, amine and hydroxyl groups will undergo a deuteron to proton back-exchange. Depending on the ^{2}H:^{1}H ratio, the ^{1}H network can be strongly diluted – for example 10 to 20 % back-exchange[2,4,6] – or fully reprotonated at all exchangeable sites[1,3,5]. Even with a 100 % back-exchange, the sample is diluted due to deuterons at non-exchangeable sites.

Figure 2

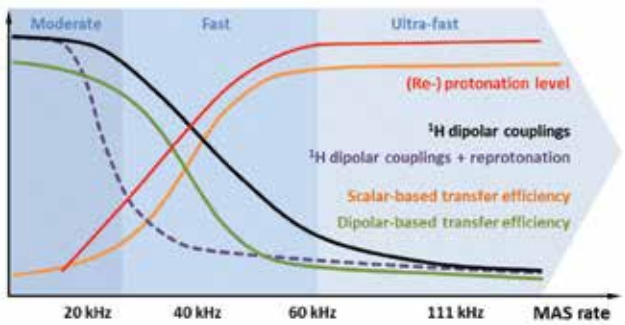

Figure 2: Schematic illustration of different aspects of protonation (red) and MAS respectively. In proportion to the MAS rate and/or reprotonation level, spectral resolution increases and longer-lived ^{13}C coherences allow the use of homonuclear scalar coupling-based polarization transfers (orange). Dipolar coupling-mediated transfer starts to become inefficient at MAS rates ≥20 kHz, due to averaging effects (green). Using strongly deuterated samples, ^{1}H dipolar couplings are already effectively attenuated at moderate MAS rates (purple). Under fast to ultra-fast rates, MAS averages out ^{1}H dipolar couplings efficiently, even in fully protonated samples (black).

Figure 3

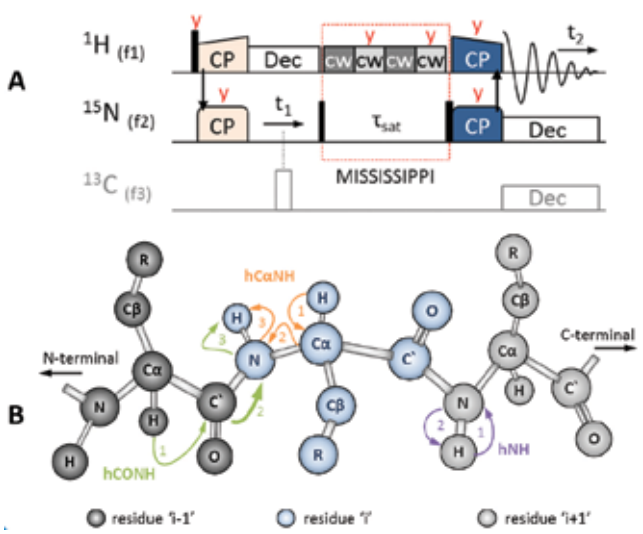

Figure 3: (A) 2D HSQC-like 'hNH2D.dcp' pulse sequence to correlate ^{15}N with ^{1}H using ^{1}H-detection. The initial ^{1}H magnetization is transferred to ^{15}N via HN CP (light orange). The ^{15}N signal evolves under ^{1}H decoupling (white). Using an H/C/N triple channel probe, ^{13}C-decoupling can also be used (gray, π hard pulse). During MISSISSIPPI water suppression (red dotted box), which is applied on-resonance with the water peak, ^{15}N magnetization is stored along Z by a π/2 hard pulse (black). Afterwards, ^{15}N magnetization is flipped back into the XY plane to transfer polarization back to ^{1}H via NH CP (dark blue), followed by ^{1}H-detection under low power decoupling on ^{15}N, and possibly ^{13}C. Pulses are applied along X, unless otherwise stated (red text). (B) Polarization transfer schemes during hNH (purple), hCαNH (orange) and hCONH (green) experiments, the latter including an interresidue sequential transfer step (thick arrow).

Increasing ^{1}H spin dilution will not only reduce unwanted dipolar couplings (Figure 2, purple), but the overall ^{1}H signal-to-noise ratio. Furthermore, selective dipolar transfer pathways may not be possible, for example due to the low propensity of two protons being in close proximity. Moreover, in the regime of fast MAS, it depends on the experimental conditions whether dipolar or scalar coupling-based experiments are preferable (Figure 2, orange and green)[3-6], and so when using fast MAS rates, experimental conditions should be carefully chosen. Alternatively, the use of strong dilution combined with moderate MAS rates[2,6] or full reprotonation under (ultra-)fast MAS[3,4], where the spinning is sufficient to weaken the ^{1}H dipolar couplings (Figure 2, red and black), is recommended.

Experiments and Pulse Programs

For ^{1}H-detected experiments, the easiest way to begin with is the heteronuclear hNH experiment, which is comparable to a solution NMR HSQC experiment, but which is based on CP. This correlates the amide proton to its nitrogen (Figure 3B, purple). Using the hCαNH sequence (Figure 3B, orange, and Figure 4A), the Cα of a residue can be correlated to the amide

Figure 4

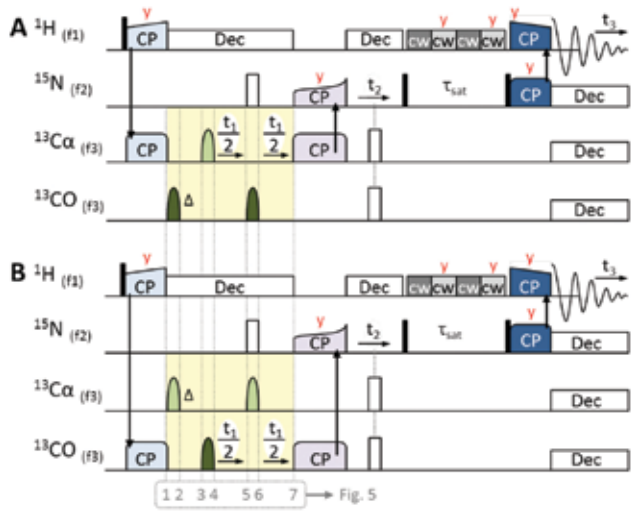

Figure 4: 3D pulse sequences of ^{1}H-detected 'hCaNH3D.tcp' (A) and 'hCONH3D.tcp' (B) for obtaining intraresidue Cα-N-H and interresidue CO-N-H correlations respectively. Initial magnetization derives from ^{1}H, followed by ^{1}H to ^{13}Cα or ^{13}CO CP (light blue). Centered during t_1, an off-resonance band-selective π pulse is used for $J_{CO-C\alpha}$ decoupling (light and dark green bell-shaped pulses). Phase evolution is compensated by a band-selective π pulse pair preceding t_1 (see Figure 5 for details). Once magnetization is transferred back to ^{15}N (purple CP step), the experiments follow the same scheme as that of the hNH experiment (Figure 3A). Pulses are applied along X unless otherwise stated (red letters).

group within the same residue. To obtain forward sequential correlations (N- to C-terminal) the hCONH (Figure 3B, green, and Figure 4B) can be used. That will correlate the backbone CO of a residue 'i-1' to the amide group of its consecutive neighbor, residue 'i'.

With the exception of 'hNH2D.dcp', the pulse sequences are applied in triple channel mode with ^{1}H on channel f1, ^{15}N on f2 and ^{13}C on f3. If the '-DTC' ('triple channel') flag is set in the TopSpin™ 'ased'-parameter 'zgoptns', the ^{13}C channel is also activated in the hNH2D.dcp (Figure 3A, gray). A detailed description of all the parameters used and the recommended conditions can be found in the header of each pulprog.

Although the three experiments yield different results, they share general pulse sequence building blocks. Initial magnetization always derives from ^{1}H excited by a π/2 hard pulse, which is followed by selective CP steps to ^{15}N (Figure 3A, orange pulses), ^{13}Cα or ^{13}CO (Figure 4, light blue pulses).

In 'hCaNH3D.tcp' and 'hCONH3D.tcp', the carrier frequency for RF irradiation (offset 'o3') is on-resonance with Cα or CO respectively. During the indirect evolution (t_1), homonuclear $J_{CO-C\alpha}$ coupling must be decoupled using a t_1-centered, band-selective π pulse, which is applied off-resonance, i.e. a CO decoupling pulse during Cα evolution in the hCαNH experiment, and *vice versa* (Figure 4, light and dark green pulses).

The off-resonance pulse causes phase evolution of the on-resonance spins, an effect often referred to as the 'Bloch-Siegert shift' in solution NMR[9] (Figure 5A, purple). Furthermore, the initial evolution time, $t_1(0)$, is greater than zero, resulting in unwanted initial chemical shift evolution for the first TD point (Figure 5A, red).

To compensate for both these effects, an on-resonance π pulse needs to precede t_1 (Figure 5A, orange). For complete refocusing (Figure 5B), a symmetry construct (Figure 4, yellow) centered around this pulse has to be created, resulting in a second off-resonance π pulse and a symmetry delay (Δ) which compensates for $t_1(0)$. Both are applied consecutive to the initial ^{1}H to ^{13}C CP.

Any other TD point is acquired with a t_1 larger than Δ, leading to desired additional chemical shift evolution, which is unaffected by refocusing (Figure 5C, cyan).

For heteronuclear decoupling (Figure 4, white pulses), a ^{15}N π hard pulse and ^{1}H low power decoupling are applied during t_1, followed by a SPECIFIC ^{13}Cα or ^{13}CO to ^{15}N CP[10,11] transfer (Figure 4, purple pulses).

Afterwards, both sequences equal the 'hNH2D.dcp' (Figure 3A), where ^{15}N evolution (t_1 or t_2) is attended by heteronuclear decoupling using a ^{13}C π hard pulse (white pulse) and ^{1}H low power decoupling.

To suppress the water signal, continuous wave (cw, dark and light gray) pulses are applied alternately along X and Y, on-resonance with the water peak.

Figure 5

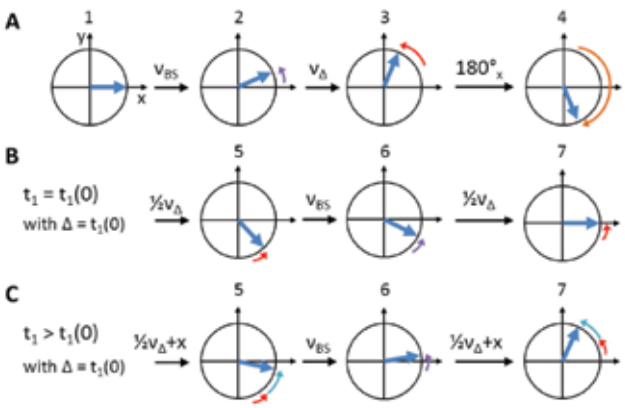

Figure 5: Schematic representation of Bloch-Siegert shift and initial t_1 ($t_1(0)$) phase evolution compensation. Numbers refer to 'hCaNH3D.tcp'/'hCONH3D.tcp' pulprog of Figure 4. (A) After the initial CP, on-resonance ^{13}C spins (blue) are oriented along X (1). The first off-resonance π pulse creates a Bloch-Siegert shift, ν_{BS}, (2, purple arrows). During the symmetry delay, Δ, which equals $t_1(0)$, additional chemical shift, ν_{Δ}, evolves (3, red arrows). Overall, evolution is reversed by the on-resonance π pulse (4, orange arrow) to refocus both ν_{BS} (6) and ν_{Δ} (5 and 7, steps of '½ν_{Δ}' are due to split t_1). While during $t_1(0)$ chemical shift evolution is refocused completely (B), it further evolves ('+x', cyan arrows) for all t_1 times larger than Δ (C).

During this so-called MISSISSIPPI H_2O suppression[12], ^{15}N magnetization is stored along Z by a π/2 hard pulse. With a second π/2 hard pulse, ^{15}N magnetization is brought back into the XY plane to transfer polarization to ^{1}H in a final ^{15}N to ^{1}H CP (dark blue pulses), followed by ^{1}H-detection under low power heteronuclear decoupling on ^{15}N and ^{13}C.

Which Experimental Conditions to Choose?

The following recommendations have been tested on a u-[^{13}C, ^{15}N]-labeled, perdeuterated and 100% ^{1}H back-exchanged ubiquitin sample at 60 kHz MAS using a Bruker 1.3 mm rotor and a Bruker Avance III HD 600 MHz Wide Bore system.

The sample temperature of approximately 294 K was regulated with a BCU II, using a N_2 gas flow of ~1,100 l/h to reach a set temperature of 257 K. Because faster MAS produces more frictional heating, the ideal sample temperature and the N_2 gas flow required should be adjusted beforehand using, for example, ^{79}Br[13]. Nevertheless, a gas flow of more than 1300 l/h should be avoided to not cause rotor imbalances at high spinning speeds. Additionally, when using temperature regulation, frame cooling should be used.

As known from 'conventional' solid-state NMR, the Hartmann-Hahn-condition $n \times \upsilon_R = \upsilon_I \pm \upsilon_S$ must be fulfilled to achieve CP transfer, with n as an integer (usually ±1 or ±2), υ_R the MAS rate and υ_I and υ_S the RF field strengths acting on the I and S spins respectively. Addition of υ_I and υ_S is known as a double-quantum (DQ) transition, and subtraction as a zero-quantum (ZQ) transition. Under (ultra-)fast MAS, selective CP is efficient already at low power irradiation, resulting in higher sensitivity for the DQ CP condition compared to ZQ (Figure 6A).

For all initial and final CP steps (ν_R = 60 kHz), RF field strengths of 50 kHz applied on ^{1}H and only 10 kHz on ^{15}N or ^{13}C, respectively, have been proven well.

SPECIFIC ^{13}C to ^{15}N CP gave best results using 35 kHz applied on ^{13}C and 25 kHz on ^{15}N. Here, the 50/ 10 kHz condition results in poor transfer efficiency and is thus not suited (Figure 6B). Nevertheless, on unknown samples it is always recommended to test different Hartmann-Hahn conditions.

During CP, the use of a shaped pulse on one of the two nuclei involved increases transfer efficiency dramatically because several Hartmann-Hahn conditions can be passed and B_1 inhomogeneity compensated (Figure 6A).[14] A shape can be applied on either of the two nuclei, while the other nucleus experiences a rectangular pulse in the form of, for example, a 'square.1000' shape.

Figure 6

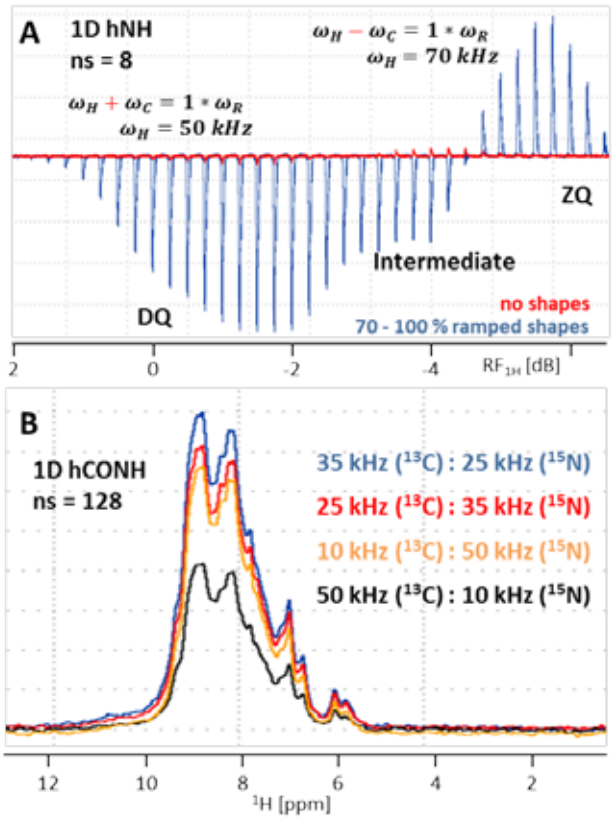

Figure 6 (A) Overlay of Hartmann-Hahn (HH) optimization curves for the initial H to N CP transfer in a 1D hNH experiment using either no shape (red) or a 70 to 100% ramp on ^{1}H (blue, 20 times more transfer efficiency). As seen in the blue curve, double-quantum (DQ) transfer yields in increased transfer efficiency by >21% compared to zero-quantum (ZQ). Because the difference is only ~3 dB, both conditions interfere causing an intermediate window with reduced signal. (B) 1D hCONH spectra with different HH conditions for the SPECIFIC CO to N CP transfer. RF field strengths of 35 kHz on ^{13}C and 25 kHz on ^{15}N (DQ condition) results in best transfer efficiency..

Here, linearly ramped up and ramped down shapes were applied on ^{1}H for all initial and final CP steps respectively. Theoretically, a flat ramp from 90 to 100 % (e.g. 'ramp9010 0.1000'/'ramp10090.1000') should perform well at high MAS rates, ensuring that magnetization is transferred during most of the contact time. However, sometimes, a steeper ramp from 70 to 100 % (e.g. 'ramp70100.1000'/'ramp10070.1000') can be more efficient, as in the presented data.

For SPECIFIC ^{13}C-^{15}N CP, a tangential amplitude modulated shape, for example 'tacn80', applied on ^{15}N is most efficient.

According to solution NMR, Gaussian pulse cascades[15] (e.g. 'Q3.2000') can be applied for 256 and 350 µs for selective 13Cα and 13CO π pulses. Note that a longer pulse is more selective. When setting the constants 'cnst21' and 'cnst22' as frequency offsets for ^{13}CO and $^{13}C\alpha$ in ppm, respectively, all necessary frequency changes are calculated and set automatically in the pulprog.

During MISSISSIPPI, the H_2O saturation time (t_{sat} in Figures 3 and 4, 'd19' in pulprogs), should be optimized between 100 and 300 ms. Cw decoupling programs (cpdprg) are called 'cwX_13nofq' and 'cwY_13nofq'. As the names imply, parameter 'plw13' is the corresponding power level, which should be set to ¼ of the MAS rate, for example 15 kHz at 60 kHz MAS.

Note: The suffix 'nofq' reveals that no frequency switch is taking place with the cpdprg itself.

Likewise, heteronuclear decoupling of only 15 kHz on ^{1}H is sufficient during $^{13}C/^{15}N$ evolution times using 'sltppm_12nofq' at power level 'plw12'.[16]

During proton acquisition, 10 kHz of heteronuclear decoupling is applied on ^{15}N and ^{13}C, using 'waltz16_16nofq' and 'waltz16_18nofq' at power levels 'plw16' and 'plw18' respectively.[17]

An overview of all necessary parameters, including recommendations, can be found in Table 1.

Outlook

In collaboration with leading scientists in the field of solid-state NMR spectroscopy, Bruker continues to implement state-of-the-art ^{1}H-detected experiments for ultra-fast MAS. Further application notes based on this introductory one will follow in the near future.

Table 1: Summary of recommended parameters for ^{1}H-detected experiments recorded at 60 kHz MAS. Parameters in bold text should be optimized. For all other parameters, it is sufficient to calculate/set the recommended values.

Parameters	Nuclei	Parameter names in pulprog	Rule of thumb
90° (180°) hard pulses	^{1}H	**p3** (p4) @ plw2	~100 kHz (2.5 µs)
	^{15}N	**p21** (p22) @ plw21	~42 kHz (6 µs), optimize in hNH2D.dcp: flag '–DN90' (zero crossing)
	^{13}C	**p1** (p2) @ plw1	~72 kHz (3.5 µs), optimize in hCxNH3D.tcp: flag '–DC90' (zero crossing)
180° selective pulses	$^{13}C\alpha$	p24* @ spw24	~350 us @ shape: 'Q3.2000'; open shape in 'shapetool> stdisp> Analysis> Integrate Shape' and enter: 'length of p24, '180.0', length of p1', result tells by how much pldb1 needs to be changed for spdb24
	^{13}CO	p23* @ spw23	~275 us @ shape: 'Q3.2000'; open shape in 'shapetool> stdisp> Analysis> Integrate Shape' and enter: 'length of p23, '180.0', length of p1', result tells by how much pldb1 needs to be changed for spdb23
CP transfers	H-N	**p25** @ **spw42** (H) & spw43 (N)	1-3 ms @ 50 kHz & 10 kHz, shapes: 'ramp90100.1000' & 'square.1000'
	H-Cα	**p18** @ **spw38** (H) & spw52 (C)	2-6 ms @ 50 kHz & 10 kHz, shapes: 'ramp90100.1000' & 'square.1000'
	H-CO	**p19** @ **spw39** (H) & spw53 (C)	2-6 ms @ 50 kHz & 10 kHz, shapes: 'ramp90100.1000' & 'square.1000'
	Cα-N	**p16** @ **spw5** (N) & spw50 (C)	3-10 ms @ 25 kHz & 35 kHz, shapes: 'tacn80' & 'square.1000'
	CO-N	**p17** @ **spw6** (N) & spw51 (C)	3-10 ms @ 25 kHz & 35 kHz, shapes: 'tacn80' & 'square.1000'
	N-H	**p45** @ **spw47** (N) & spw46 (H)	400-800 µs @ 50 kHz & 10 kHz, shapes: 'square.1000' & 'ramp10090.1000'
Decoupling	^{1}H	cpdprg1 @ pcpd1 & plw12	'sltppm_12nofq' @ 33.33 µs & ¼ * ν_R (15 kHz)
		cpdprg4/5 @ **d19** & plw13	'cwX_13nofq'/ 'cwY_13nofq' @ 100-300 ms & 15 kHz (=MISSISSIPPI)
	^{15}N	cpdprg2 @ pcpd2 & plw16	'waltz16_16nofq' @ 25 µs & 10 kHz
	^{13}C	cpdprg3 @ pcpd3 & plw18	'waltz16_18nofq' @ 25 µs & 10 kHz
Offsets	^{1}H	o1	on resonance with the water peak (~5 ppm)
	^{15}N	o2	center of ^{15}N signal (~119 ppm)
	^{13}C	o3 (hCαNH3D.tcp)	on resonance with Cα region (~54 ppm)
		o3 (hCONH3D.tcp)	on resonance with CO region (~174 ppm)
		cnst21	frequency offset for CO (~174 ppm)
		cnst22	frequency offset for Cα (~54 ppm)
		cnst26	frequency offset for CO-Cα (~114 ppm)

* The pulse length is linearly proportional to $1/B_0$.

References

1. B. Reif et al., ^{1}H-^{1}H MAS Correlation Spectroscopy and Distance Measurements in a Deuterated Peptide. *J Magn Reson* (2001) 151:320–327.
2. V. Chevelkov et al., Ultrahigh Resolution in Proton Solid-State NMR Spectroscopy at High Levels of Deuteration. *Angew Chem Int Ed* (2006) 118:3963-3966.
3. M.J. Knight et al., Fast Resonance Assignment and Fold Determination of Human Superoxide Dismutase by High-Resolution Proton-Detected Solid-State MAS NMR Spectroscopy. *Angew Chem Int Ed* (2011) 50:11697-11701.
4. D.H. Zhou et al., Solid-state NMR analysis of membrane proteins and protein aggregates by proton detected spectroscopy. *J Biomol NMR* (2012) 54:291-305.
5. E. Barbet-Massin et al., Rapid Proton-Detected NMR Assignment for Proteins with Fast Magic Angle Spinning. *J Am Chem Soc* (2014) 136:12489-12497.
6. V. Chevelkov et al., Proton-detected MAS NMR experiments based on dipolar transfers for backbone assignment of highly deuterated proteins. *J Magn Reson* (2014) 242:180-188.
7. D.P. Burum & R.R. Ernst, Net polarization transfer via a J-ordered state for signal enhancement of low-sensitivity nuclei. *J Magn Reson* (1980) 39:163-168.
8. S.R. Hartmann & E.L. Hahn, Nuclear Double Resonance in the Rotating Frame. *Phys Rev* (1962) 128:2042-2053.
9. F. Bloch & A. Siegert, Magnetic Resonance for Nonrotating Fields. *Phys Rev* (1940) 57:522-527.
10. M. Baldus et al., Efficient ^{15}N-^{13}C Polarization Transfer by Adiabatic-Passage Hartmann-Hahn Cross Polarization. *J Magn Reson* (1996) 118:140-144.
11. M. Baldus et al., Cross polarization in the tilted frame: assignment and spectral simplification in heteronuclear spin systems. *Mol Phys* (1998) 95:1197-1207.
12. D.H. Zhou & C.M. Rienstra, High-Performance Solvent Suppression for Proton-Detected Solid-State NMR. *J Magn Reson* (2008) 192:167-172.
13. K.R. Thurber et al., Measurement of sample temperatures under magic-angle spinning from the chemical shift and spin-lattice relaxation rate of 79Br in KBr powder. *J Magn Reson* (2009) 196:84-87.
14. O.B. Peersen et al., Variable-Amplitude Cross-Polarization MAS NMR. *Magn Reson* (1993) 104:334-339.
15. L. Emsley & G. Bodenhausen, Gaussian pulse cascades – new analytical functions for rectangular selective inversion and in-phase excitation in NMR. *Chem Phys Lett* (1990) 165:469-476.
16. J.R. Lewandowski et al., Measurement of Site-Specific 13C Spin-Lattice Relaxation in a Crystalline Protein. *J Am Chem Soc* (2010) 132:8252-8254.
17. A.J. Shaka et al., An improved sequence for broadband decoupling: WALTZ-16. *J Magn Reson* (1983) 52:335-338.

www.bruker.com **Bruker BioSpin**
info@bruker.com